Remote Sensing Letters

ISSN: 2150-704X (Print) 2150-7058 (Online) Journal homepage: www.tandfonline.com/journals/trsl20

The visible built-up index: advancing the detection of high-albedo urban areas

Weizhi Li, Aiyin Zhang & Florencia Sangermano

To cite this article: Weizhi Li, Aiyin Zhang & Florencia Sangermano (2026) The visible built-up index: advancing the detection of high-albedo urban areas, Remote Sensing Letters, 17:2, 123-131, DOI: 10.1080/2150704X.2025.2609845

To link to this article: https://doi.org/10.1080/2150704X.2025.2609845

REMOTE SENSING LETTERS
2026, VOL. 17, NO. 2, 123–131
https://doi.org/10.1080/2150704X.2025.2609845

Taylor & Francis
Taylor & Francis Group

The visible built-up index: advancing the detection of high-albedo urban areas

Weizhi Li [a], Aiyin Zhang [a] and Florencia Sangermano [a,b]

[a]Graduate School of Geography, Clark University, Worcester, MA, USA; [b]Clark Center for Geospatial Analytics, Worcester, MA, USA

ABSTRACT

This study introduces the Visible Built-up Index (VBI), a novel spectral index derived from the visible bands of Sentinel-2 satellite imagery. VBI is designed to enhance the extraction of built-up areas, particularly in regions dominated by high-albedo building materials. The index was evaluated against 11 other spectral indices. Our statistical and visual assessments demonstrate that VBI outperforms existing indices in detecting built-up surfaces, with area under the total operating characteristic curve (TOC AUC) values for VBI = 0.97, NDBI = 0.808 and BU = 0.916. VBI effectively highlights highly reflective roofs, distinguishes water bodies and vegetation from built-up areas, and partially separates bare soil from urban regions. Because VBI relies solely on visible bands, it enables built-up area extraction from Sentinel-2 imagery at 10 m resolution. Moreover, its simplicity broadens its applicability across various sensors, historical datasets, and drone platforms.

ARTICLE HISTORY
Received 11 March 2025
Accepted 19 December 2025

KEYWORDS
Urban detection; Built-up index; Córdoba

1. Introduction

With the swift expansion of urban areas, the identification of built-up areas through remote sensing is crucial to assess their impact across multiple scales. Impervious surfaces, such as roads, parking lots, and rooftops, are the core components of built-up areas. These surfaces prevent water from infiltrating into the soil, affecting watershed runoff and contributing to environmental impacts such as urban heat islands, habitat degradation, deforestation, and public health issues (Weng 2012).

Remote sensing (RS) technology is a valuable tool for monitoring built-up land dynamics given its ability to provide timely and cost-effective data (Xu 2008). Numerous studies have proposed various built-up indices, which exploit the high shortwave infrared (SWIR) and low near-infrared (NIR) reflectance of built-up surfaces, to segment and map urban areas. For instance, Zha, Gao, and Ni (2003) introduced the Normalized Difference Built-up Index (NDBI) using NIR and SWIR and emphasized that NDBI should be combined with the Normalized Difference Vegetation Index (NDVI) to improve built-up area extraction. Building on this approach, He et al. (2010) modified the method and proposed the Built-up Index (BU). In addition, other indices, including Index-Based Built-up Index (IBI),

CONTACT Florencia Sangermano fsangermano@clarku.edu Graduate School of Geography, Clark University, 950 Main St, Worcester, MA 01610, USA
Supplemental data for this article can be accessed online at https://doi.org/10.1080/2150704X.2025.2609845.

New Built-up Index (NBI), Normalized Built-up Area Index (NBAI), Built-up and Bare-land area Index (BBI), Built-up Area Extraction Index (BAEI), and Impervious Built-up Index (IBUI), have been applied in different regions of the world, generally performing well under their respective urban conditions (Bouzekri, Aziz Lasbet, and Lachehab 2015; Jieli et al. 2010; Santra et al. 2020; Waqar et al. 2012; Xu 2008; Zhou et al. 2014). However, most of these indices rely on a SWIR band, which in the case of Sentinel-2 it is provided at a coarser resolution. Moreover, many high-resolution satellites and drone platforms either lack these bands or acquiring them incurs extra costs, limiting the application of those indices for detailed urban mapping.

In this study, we propose a built-up index derived solely from the transformation of visible bands into HSV space, providing a straightforward and effective approach for mapping bright surface built-up areas. Unlike traditional indices, it does not depend on NIR or SWIR bands, making it suitable for high-resolution sensors.

2. Methods

2.1. Study area

The development of this index was targeted at the extraction of urban areas within the Capital Department of *Córdoba*, in central Argentina, as the delineation was required for the assessment of the spread of vector mosquitoes. A previous study utilized NDBI to assess urban density in *Córdoba* for epidemiological research (Estallo et al. 2018); however, the results showed poor built-up area extraction, which motivated the development of this new index. The urban area within this district is dominated by high-albedo roofing materials, mainly concrete (Figure 1), and the development of our index was targeted for those conditions. The study area covers approximately 600 km^2, with the *Suquía* River running through the built-up centre, surrounded by vegetation, agricultural, and bare land. Areas of high population density present high-albedo roofing materials, such as cement, concrete, and silver colour metal roofs. Terracotta-clay tiled red roofs are the second most common roofing type, which are more prevalent in suburban neighbourhoods. In these suburban areas, houses are sparsely distributed and surrounded by dense vegetation, and the urban area is surrounded by fallow fields and croplands.

2.2. Image pre-processing and index calculation

Previous studies have recommended using summertime imagery for identifying impervious surfaces due to the less noticeable changes in plant phenology and less likely mixing of space characteristics (Weng, Hu, and Liu 2009). We downloaded from Google Earth Engine Sentinel-2 Harmonized collection, a cloud-free image from 24 January 2024. High-albedo roofing materials exhibit high reflectance in all spectral bands (Figure S2a), here we call these 'white roofs'. Water has low reflective properties across all bands, as water absorbs most radiation across these wavelengths. Vegetation has low reflectance in the visible bands, a peak in the NIR band, and a decrease in the SWIR bands. Bare soil and other built-up types (e.g., asphalt road, red and other roofs, and cement/concrete ground surfaces) exhibit similar spectral trends, making it difficult to distinguish between them using spectral bands.

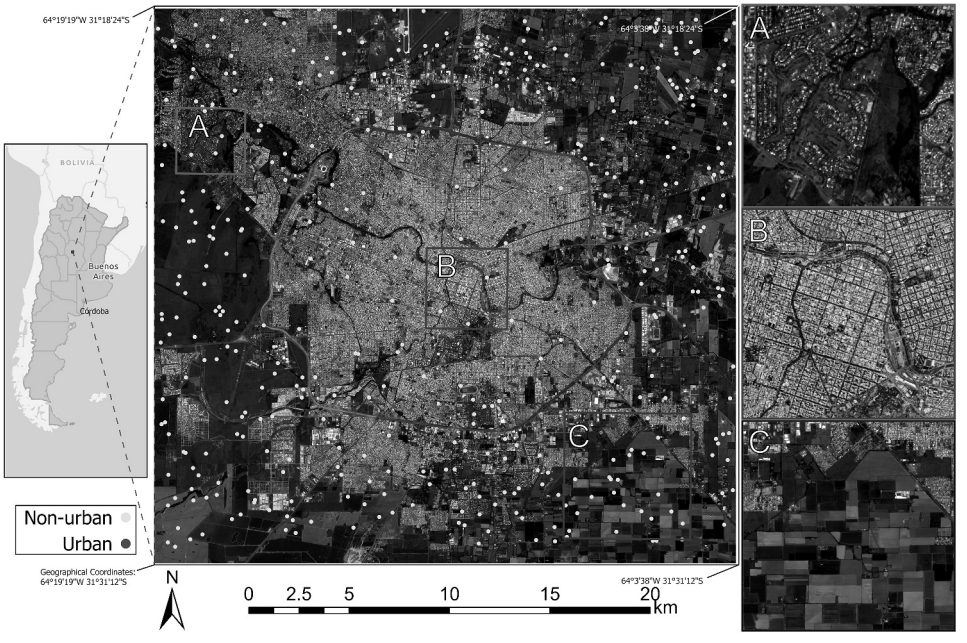

Figure 1. Capital Department of *Córdoba*, Argentina, in 24 January 2024. Points show 615 sample pixels used for validation. Focus window A, is a suburban area, where houses are sparsely distributed and surrounded by dense vegetation. Terracotta-clay tiled roofs, which we call red roofs, are more prevalent in suburban areas. Window B depicts an area of high population density, with predominantly high-albedo roofing materials, such as white cement and silver colour metal roofs. Window C shows fallow fields and croplands, offering insight into non-urban land cover. Colour picture in supporting information.

To facilitate the distinction across urban materials, we transformed the visible red, green, and blue bands into the hue, saturation, and value (HSV) colour space. In the HSV space (Figure S2b), the saturation and value bands were more effective at distinguishing among various land cover types compared to the optical or infrared bands. HSV colour transformation has been applied to enhance waterbody delineation (Namikawa, Sehn Körting, and Ferreira Castejon 2016), however, to our knowledge, it has not been applied to detect built-up areas.

Recognizing the distinct contrast between saturation and value across various land cover categories and the opposite signature pattern for white roofs and light backgrounds (Figure S2), we developed a built-up index using a normalized difference formula on the Value and Saturation components of the HSV colour transformation (Table S3). We term this index the Visible Built-up Index (VBI). Sentinel-2 bands for the red (band 4), green (band 3), and blue (band 2) parts of the electromagnetic spectrum were used to generate the VBI at 10 m resolution. VBI ranges from −1 to 1, where positive values indicate the presence of built-up surfaces.

VBI's performance was compared against 11 indices (see details in supporting information). Given that the main objective of this communication is to present VBI, and to keep the manuscript concise, we only present in detail the comparison to NDBI (Zha, Gao, and Ni 2003) and BU (He et al. 2010) as they are the most cited built-up indices.

2.3. Built-up index evaluation

In order to validate the built-up indices, 615 randomly sampled pixels (Figure 1) were selected as reference. We visually inspected and categorized these 615 reference samples into two classifications. Level I classification distinguished between non-built-up and built-up without further categorization of the land cover. Level II refined the categorization of the reference samples into vegetation, water, bare soil, white roofs, red roofs, other roof types, asphalt roads, and cement cover, to ensure they are mutually exclusive and collectively exhaustive (Table S1).

We used the total operating characteristic (TOC) method and the area under the TOC curve (AUC) to assess and compare the performance of these three built-up indices (Pontius and Si 2014, Pontius and Parmentier 2014). The Minimum Quantity Difference (MQD) approach was applied to determine the optimal threshold for each index. Each index was then thresholded at its optimal value to produce built-up maps, enabling direct comparison of spatial allocation differences while keeping the total mapped built-up areas constant (Liu and Pontius 2021).

The Mann–Whitney U test was used to compare index values between built-up and non-built-up at reference sampled locations, while Kruskal–Wallis with Dunn's post-hoc tests were used to compare index values across the level II land cover types (Alexis 2014; McKnight and Najab 2010).

3. Results

NDBI presented a relatively homogeneous distribution of values across the study area, with built-up regions displaying slightly higher values than non-built-up areas, and less contrast compared to BU and VBI. BU presented a clearer distinction between built-up and vegetated areas, with higher values observed in the urban core. However, high values were also present in bare lands, such as fallow fields in the southeastern and southwestern regions. VBI enhanced the visibility of high-albedo surfaces, with built-up areas showing higher values, while vegetation and waterbodies were deemphasized compared to the other indices (Figure 2).

All indices were capable of discriminating built-up pixels from non-built up (Figure S3), with VBI having the best diagnostic ability (AUC = 0.97), followed by BU (AUC = 0.916), and

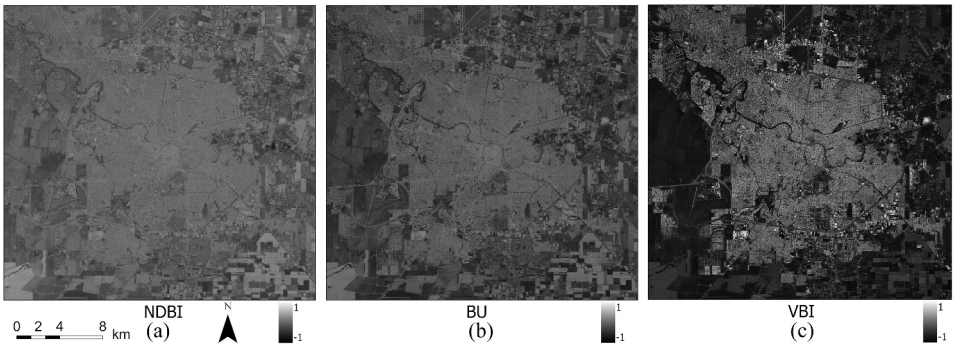

Figure 2. NDBI (a), BU (b), and VBI (c) in the study area at the range from −1 to 1.

Table 1. The contingency table at the optimal threshold of NDBI, BU, and VBI.

		Reference		
		Presence	Absence	Sum
NDBI = −0.002				
Diagnosis	Presence	128	77	205
	Absence	77	333	410
	Sum	205	410	615
BU = −0.14				
Diagnosis	Presence	154	51	205
	Absence	51	359	410
	Sum	205	410	615
VBI = −0.373				
Diagnosis	Presence	178	27	205
	Absence	27	383	410
	Sum	205	410	615

NDBI (AUC = 0.808). At the optimal threshold for each index (Table 1) VBI correctly classified 86.83% of built-up reference samples; with declining performance for BU and NDBI (75.12% and 62.44% correctly classified respectively).

The spatial distribution of built-up regions varies greatly across the indices (Figure 3). All indices effectively captured the highly dense built-up areas, but NDBI (Figure 3a) and BU (Figure 3b) misclassified some bare soil as built-up. Both NDBI and BU confused bare lands with built-up areas (Figure S4.a). Although VBI classified some dry bright soils as built-up, it correctly distinguished most bare soil types from built-up areas. BU also misclassified some ponds as built-up, NDBI classified pond edges as built-up, but VBI correctly identified them as non-built-up. All indices successfully classified major built-up areas (Figure S4.b.) and distinguished non-built-up features, such as rivers and trees. However, red-roofed buildings were not well detected by VBI. Additionally, asphalt roads were overlooked by VBI, likely due to the shadows and trees affecting classification. In suburban areas, where buildings are sparsely distributed and surrounded by dense

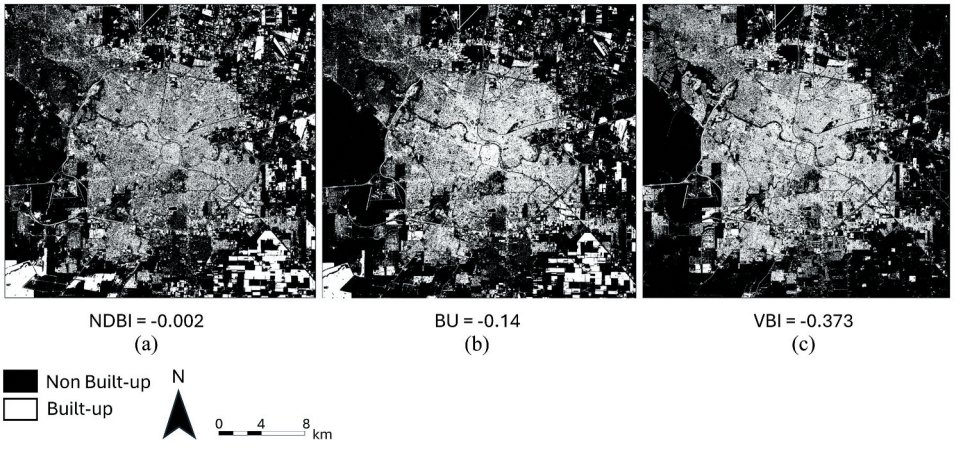

Figure 3. Binomial built-up and non-built-up classification derived from applying the optimal threshold to NDBI (a), BU (b), and VBI (c) in the study area. Black: non-built-up areas, white: built-up areas.

vegetation (Figure S4.c), NDBI and BU identified some of built-up structures, but VBI provides a better performance. VBI effectively outlined the building structures against the vegetation background.

All indices were able to differentiate built-up pixels from non-built-up pixels ($p < 0.01$) with VBI having a stronger diagnostic ability for separating built-up areas from non-built-up (Figure S5).

In general, VBI index values are well distributed across the full index range, while BU and NDBI had less variability (Figure S6). The VBI index exhibited the highest number of significant ($p < 0.05$) pairwise differences in index values compared to BU and NDBI (Figure 4). VBI was capable of separating ($p < 0.01$) built land covers (white roofs, red, roofs, other roofs, roads, and cement ground) from almost all non-built land cover types (vegetation, water, and soil), with the exception for red roofs and roads not being different from bare soil.

BU and NDBI had limited statistical differences between built-up and non-built-up classes. NDBI and BU were capable of separating vegetation from built-up classes ($p < 0.01$). While BU was capable of separating white roofs from soil and water ($p < 0.05$), NDBI was not capable of this distinction. Similar to VBI, neither BU nor NDBI was able to separate red roofs from bare soil.

In addition to BU and NDBI, nine other built-up indices – IBI, BBI, IBUI, BAEI, Band Ratio for Built-up Area (BRBA), Vegetation Index Built-up Index (VIBI), NBI, NBAI, and Multi-index Built-up Index (MultiBI) (Osgouei et al. 2019; Santra et al. 2020; Stathakis, Perakis, and Savin 2012) – were evaluated against VBI (see supporting information). Although all indices were capable of separating general built-up vs non-built-up classes (Figure S8), VBI outperformed all indices under the current urban setting characterized by high-albedo surfaces (Table S4). There is substantial variability in the land cover types that each index can distinguish (Figure S9, Figure S10). The most consistent pattern across indices is their ability to separate built-up areas from vegetation and water. BAEI (Bouzekri, Aziz Lasbet, and Lachehab 2015) is the only index that fails to separate vegetation from roads or clay roofing materials ('red' roofs). Seven out of the twelve indices compared (Figure S9) successfully separated built-up surfaces from water. We note that VBI performed nearly identically to NBAI (Table S4), with only minimal improvements. VBI values for terracotta

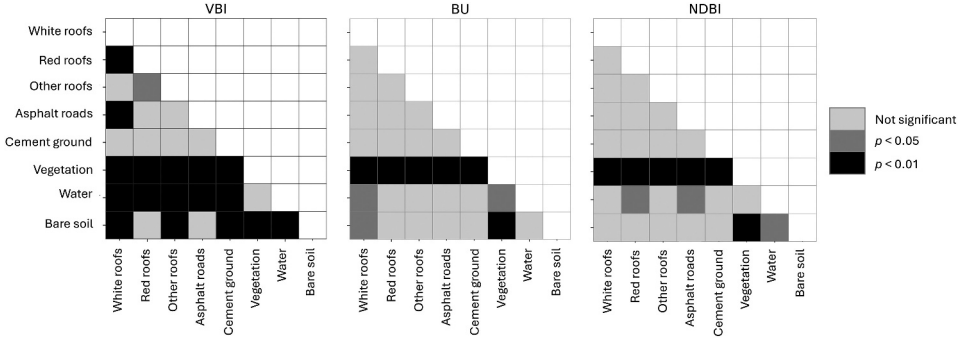

Figure 4. Triangular statistical significance matrices from Dunn's post-hoc test for VBI, BU, and NDBI. Black cells show significant differences at 99% confidence ($p < 0.01$), Dark grey cells show significant differences at 95% confidence ($p < 0.05$). Light grey denotes non-significant differences ($p \geq 0.05$).

clay roofing materials ('red' roofs) were significantly different ($p < 0.05$, Figure S9) from the index values of other roofing materials ('other' roofs), whereas NBAI values did not show a significant difference between these two classes. BBI (Zhou et al. 2014) is the only index, besides the one presented in this manuscript, that relies solely on visible bands, however its performance was relatively low, with an AUC of 0.776 and a per cent accuracy of 58.54% at the optimal threshold. BBI could separate water and vegetation from built-up covers but was not able to separate soil from white or other roof types. In general, all indices had some difficulty separating bare fallow soils from built-up areas (example in Figure S7), but VBI and NBAI better discrimination of this class (Figure S10).

4. Discussion and conclusions

We proposed the Visible Built-up Index (VBI) based on the HSV transformation of the visible bands of Sentinel-2 imagery. VBI was able to separate built-up surfaces from water bodies, bare soil, and vegetation, and improving the detection of built-up areas and outperforming all indices assessed.

The main advantage of VBI over other indices lies in its reliance solely on visible bands, enabling its application to a wide range of high spatial resolution optical imagery with limited spectral coverage. For example, Sentinel-2 imagery provides visible and near-infrared bands at a spatial resolution of 10 m, while shortwave infrared (SWIR) bands are available at 20 m resolution. All indices – except for BBI – require the SWIR band and therefore cannot be generated at spatial resolutions finer than 20 m. BBI, shares this advantage, however fell short at separating built-up classes (white roofs, red roofs, other roofs, roads) from other land cover types besides vegetation and water. VBI outperformed all other indices evaluated for our case study in *Córdoba*, Argentina – a district with high reflective urban surfaces intermixed with water and surrounded by fallow agricultural fields.

The main limitation of all indices is the separation of terracotta clay roofs and roads, from bare fallow soils, underscoring a further gap for future research. Given the heterogeneity of construction materials and land cover types surrounding and intermixed with urban areas, this work emphasizes the importance of assessing the reflectance properties of urban features before selecting an appropriate built-up index for urban detection and classification.

Acknowledgments

The authors would like to thank the two anonymous reviewers for their thoughtful and constructive feedback, which helped improve the clarity and rigour of this manuscript.

Disclosure statement

No potential conflict of interest was reported by the author(s).

ORCID

Weizhi Li http://orcid.org/0009-0002-8504-4581

Aiyin Zhang http://orcid.org/0000-0001-6236-7105
Florencia Sangermano http://orcid.org/0000-0003-4437-4293

Data availability statement

The imagery used in this study is available through Python. Code and validation set can be found in https://github.com/vanchy-li/VBI/tree/Wins.

References

Alexis, D. 2014. "Dunn.Test: Dunn's Test of Multiple Comparisons Using Rank Sums." https://doi.org/10.32614/CRAN.package.dunn.test

Bouzekri, S., A. Aziz Lasbet, and A. Lachehab. 2015. "A New Spectral Index for Extraction of Built-Up Area Using Landsat-8 Data." *Journal of the Indian Society of Remote Sensing* 43 (4): 867–873. https://doi.org/10.1007/s12524-015-0460-6

Estallo, E. L., F. Sangermano, M. Grech, F. Ludueña-Almeida, M. Frías-Cespedes, M. Ainete, W. Almirón, and T. Livdahl. 2018. "Modelling the Distribution of the Vector Aedes Aegypti in a Central Argentine City." *Medical and Veterinary Entomology* 32 (4): 451–461. https://doi.org/10.1111/mve.12323

He, C., P. Shi, D. Xie, and Y. Zhao. 2010. "Improving the Normalized Difference Built-Up Index to Map Urban Built-Up Areas Using a Semiautomatic Segmentation Approach." *Remote Sensing Letters* 1 (4): 213–221. https://doi.org/10.1080/01431161.2010.481681

Jieli, C., L. Manchun, L. Yongxue, S. Chenglei, and H. Wei. 2010 "Extract Residential Areas Automatically by New Built-up Index." *18th International Conference on Geoinformatics*, Beijing, China, 1–5. IEEE. https://doi.org/10.1109/GEOINFORMATICS.2010.5567823

Liu, Z., and R. G. Pontius Jr. 2021. "The Total Operating Characteristic from Stratified Random Sampling with an Application to Flood Mapping." *Remote Sensing* 13 (19): 3922. https://doi.org/10.3390/rs13193922

McKnight, P. E., and J. Najab. 2010. "Mann-Whitney U Test." In *The Corsini Encyclopedia of Psychology*, edited by I. B. Weiner and W. E. Craighead, 1–1. 1st ed. Wiley. https://doi.org/10.1002/9780470479216.corpsy0524

Namikawa, L. M., T. Sehn Körting, and E. Ferreira Castejon. 2016. "Water Body Extraction from RapidEye Images: An Automated Methodology Based on Hue Component of Color Transformation from RGB to HSV Model." *Revista Brasileira de Cartografia* 68 (6). https://doi.org/10.14393/rbcv68n6-44495

Osgouei, E., S. K. Paria, E. Sertel, and U. Alganci. 2019. "Separating Built-Up Areas from Bare Land in Mediterranean Cities Using Sentinel-2A Imagery." *Remote Sensing* 11 (3): 345. https://doi.org/10.3390/rs11030345

Pontius, R. G., and B. Parmentier. 2014. "Recommendations for Using the Relative Operating Characteristic (ROC)." *Landscape Ecology* 29 (3): 367–382. https://doi.org/10.1007/s10980-013-9984-8

Pontius, R. G., Jr, and K. Si. 2014. "The Total Operating Characteristic to Measure Diagnostic Ability for Multiple Thresholds." *International Journal of Geographical Information Science* 28 (3): 570–583. https://doi.org/10.1080/13658816.2013.862623

Santra, A., S. Santra Mitra, S. Sinha, and S. Routh. 2020. "Performance Testing of Selected Spectral Indices in Automated Extraction of Impervious Built-Up Surface Features Using Resourcesat LISS-III Image." *Arabian Journal of Geosciences* 13 (22): 1229. https://doi.org/10.1007/s12517-020-06183-z

Stathakis, D., K. Perakis, and I. Savin. 2012. "Efficient Segmentation of Urban Areas by the VIBI." *International Journal of Remote Sensing* 33 (20): 6361–6377. https://doi.org/10.1080/01431161.2012.687842

Waqar, M. M., J. Fatimah Mirza, R. Mumtaz, and E. Hussain. 2012. "Development of New Indices for Extraction of Built-Up Area & Bare Soil from Landsat Data." *Open Access Scientific Reports* 1 (1): 4.

Weng, Q. 2012. "Remote Sensing of Impervious Surfaces in the Urban Areas: Requirements, Methods, and Trends." *Remote Sensing of Environment* 117 (February): 34–49. https://doi.org/10.1016/j.rse.2011.02.030

Weng, Q., X. Hu, and H. Liu. 2009. "Estimating Impervious Surfaces Using Linear Spectral Mixture Analysis with Multitemporal ASTER Images." *International Journal of Remote Sensing* 30 (18): 4807–4830. https://doi.org/10.1080/01431160802665926

Xu, H. 2008. "A New Index for Delineating Built-Up Land Features in Satellite Imagery." *International Journal of Remote Sensing* 29 (14): 4269–4276. https://doi.org/10.1080/01431160802039957

Zha, Y., J. Gao, and S. Ni. 2003. "Use of Normalized Difference Built-Up Index in Automatically Mapping Urban Areas from TM Imagery." *International Journal of Remote Sensing* 24 (3): 583–594. https://doi.org/10.1080/01431160304987

Zhou, Y., G. Yang, S. Wang, L. Wang, F. Wang, and X. Liu. 2014. "A New Index for Mapping Built-Up and Bare Land Areas from Landsat-8 OLI Data." *Remote Sensing Letters* 5 (10): 862–871. https://doi.org/10.1080/2150704X.2014.973996